Road-Adaptive Fuzzy-LQR Control for a Quarter-Car Active Suspension System

Hoa Thi Thanh Lai
Thai Nguyen University of Technology, Vietnam
laithithanhhoa@tnut.edu.vn (corresponding author)

K. L. Lai
Thai Nguyen University of Technology, Vietnam
laikhaclai@tnut.edu.vn

Trung Ngoc Dang
Thai Nguyen University of Technology, Vietnam
dotrunghai@tnut.edu.vn

Received: 2 March 2026 | Revised: 6 April 2026 | Accepted: 17 April 2026

 DOI: https://doi.org/10.48084/etasr.18475

ABSTRACT

This study presents an Adaptive Fuzzy–Linear Quadratic Regulator (AF–LQR) controller for a quarter active suspension of a vehicle operating under both stochastic road excitation and ISO 8608. The proposed method integrates a conventional LQR feedback structure with a bounded gain adaptation mechanism to adjust the control intensity according to the suspension deflection and body acceleration levels. Road turbulence was modeled using the ISO 8608 Power Spectral Density (PSD) to reflect the actual driving conditions. The simulation results show that the proposed controller significantly reduces the RMS body acceleration compared with the passive suspension and improves vibration attenuation compared with the classic LQR, while keeping the suspension deflection within safe limits. Compared with the H∞ control, the AF–LQR achieved a more balanced compromise between driving comfort and actuator force requirement, avoiding overly aggressive control actions. Robustness analysis under ±20% parameter variations confirmed stable and consistent performance. The results prove that the AF–LQR is an efficient and computationally lightweight solution for active suspension under real road conditions.

Keywords-active suspension; adaptive fuzzy control; LQR; H∞ control; ISO 8608; quarter-car model

I. INTRODUCTION

Active suspension systems play a crucial role in modern automotive engineering by improving ride comfort, road holding, and overall vehicle stability under uncertain road disturbances [1-4]. In practice, suspension control is inherently a multi-objective problem, requiring a balance between minimizing body acceleration, limiting suspension deflection, and maintaining tire-road contact under varying operating conditions [2-3].

Classical control strategies, including PID-based and conventional damping approaches, have been widely studied due to their simplicity and ease of implementation [5]. However, their performance is often limited by strong disturbances, nonlinearities, and parameter uncertainties.

Optimal control methods, particularly Linear Quadratic Regulator (LQR), provide a systematic framework to balance performance and control effort and have been extensively applied in suspension systems [6-7]. Nevertheless, fixed-gain LQR controllers exhibit limited adaptability when system parameters vary or road conditions change [8].

To overcome these limitations, adaptive and robust control approaches have been developed to enhance system performance under uncertainties [9-11]. Although effective, these methods often introduce increased control effort or computational complexity, which may limit real-time implementation in embedded automotive systems [12-13].

Intelligent and optimization-based control strategies, including estimation-based, data-driven, and multi-objective optimization approaches, have attracted increasing attention owing to their ability to handle nonlinear and time-varying dynamics [14-16]. However, many of these approaches rely on complex structures and lack explicit stability guarantees.

In practical automotive applications, road excitations are stochastic and are commonly modeled using ISO 8608 Power Spectral Density (PSD) descriptions. Evaluating suspension performance under ISO-standard road profiles is essential for realistic assessments and vibration analyses [17]. However,

many studies still rely on simplified excitations, limiting their practical relevance.

Advanced control and learning-based approaches have been explored to improve suspension performance under realistic driving conditions [18-19]. In addition, simulated road profile generation based on ISO standards has been widely adopted for performance evaluation in vibration analyses [20].

Motivated by these limitations, this study proposes an Adaptive Fuzzy– Linear Quadratic Regulator (AF–LQR) control strategy that integrates the optimal structure of LQR with a bounded fuzzy-based gain adaptation mechanism. The proposed approach adjusts control intensity in real time according to suspension deflection and body acceleration, thereby improving adaptability under varying road conditions while maintaining low computational complexity.

II. QUARTER CAR SUSPENSION MODEL

Figure 1 presents the two-degree-of-freedom quarter-car model composed of the sprung mass m_s (kg) and unsprung mass m_u (kg). The suspension between the two masses is modeled using a linear spring k_s(N/m) and a viscous damper b_s(Ns/m). The tire is represented by stiffness k_t(N/m), whereas tire damping b_t(Ns/m) is neglected for simplicity.

The active actuator generates a control force f_s(N) between m_s and m_u, regulated by the AF-LQR controller. The vertical displacements of the sprung and unsprung masses are denoted by x_s(m) and x_u(m), respectively, and the road disturbance is modeled as $r(t)$(m).

Applying Newton's second law to the sprung and unsprung masses yields:

$$\begin{cases} m_s\ddot{x}_s = -k_s\left(x_s - x_u\right) - b_s\left(\dot{x}_s - \dot{x}_u\right) + u \\ m_u\ddot{x}_w = k_s\left(x_s - x_u\right) + b_s\left(\dot{x}_s - \dot{x}_u\right) - k_t\left(x_u - w\right) - u \end{cases} \quad (1)$$

where x_s is the vertical displacement of the sprung mass (m), x_u is the vertical displacement of the unsprung mass (m), $\dot{x}_s$ is the velocity of the sprung mass (m/s), and $\dot{x}_u$ is the velocity of the unsprung mass (m/s).

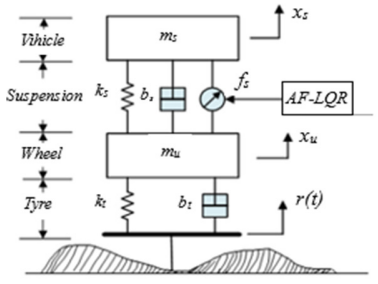

Fig. 1. Basic structure of the quarter-car active suspension system.

The state vector is selected as: $x = \left[x_s, \dot{x}_s, x_u, \dot{x}_u\right]^T$

and the system can be represented in the state-space form as:

$$\dot{x} = Ax + B_u u + B_w w \quad (2)$$

where A, B_u, and B_w denote the system matrices:

$$A = \begin{bmatrix} 0 & 1 & 0 & 0 \\ -\frac{k_s}{m_s} & -\frac{b_s}{m_s} & \frac{k_s}{m_s} & \frac{b_s}{m_s} \\ 0 & 0 & 0 & 1 \\ \frac{k_s}{m_u} & \frac{b_s}{m_u} & -\frac{k_s + k_t}{m_u} & -\frac{b_s}{m_u} \end{bmatrix}$$

$$B_u = \begin{bmatrix} 0 & \frac{1}{m_s} & 0 & -\frac{1}{m_u} \end{bmatrix}^T$$

$$B_w = \begin{bmatrix} 0 & 0 & 0 & \frac{k_t}{m_u} \end{bmatrix}$$

The performance outputs are selected as:

$$z = \left[x_s,\ x_s - x_u,\ \ddot{x}_s\right]^T$$

corresponding to ride comfort, suspension travel limitation, and body acceleration, respectively:

$$z = Cx + D_u u \quad (3)$$

where C and D_u are defined as:

$$C = \begin{bmatrix} 1 & 0 & 0 & 0 \\ 1 & 0 & -1 & 0 \\ -\frac{k_s}{m_s} & -\frac{b_s}{m_s} & \frac{k_s}{m_s} & \frac{b_s}{m_s} \end{bmatrix}$$

$$D_u = \begin{bmatrix} 0 \\ 0 \\ \frac{1}{m_s} \end{bmatrix}$$

III. CONTROLLER DESIGN

The quarter-car suspension system is considered in state-space form as:

$$\dot{x} = Ax + B_u u + B_w w, \quad z = C_z x + D_{zu} u \quad (4)$$

where $x \in \mathbb{R}^4$ is the state vector, $u = f_s$ is the control force, and $w = r(t)$ is the road disturbance input.

The performance vector z is defined to reflect the control objectives, including suspension deflection, body acceleration, and control effort.

Three control strategies were investigated: classical LQR, H∞ control, and the proposed AF–LQR controller.

A. Classical LQR Controller

The LQR problem is formulated to minimize the quadratic cost function:

$$J = \int_0^\infty \left(x^T Q x + u^T R u \right) dt \quad (5)$$

where $Q \succeq 0$ and $R \succ 0$ là are weighting matrices that define the trade-off between control performance and actuation energy.

The optimal state-feedback control law is given by:

$$u = -Kx \quad K = R^{-1} B_u^T P \quad (6)$$

where P is the positive definite solution of the algebraic Riccati equation:

$$A^T P + PA - PB_u R^{-1} B_u^T P + Q = 0 \quad (7)$$

The weighting matrices are normalized according to the desired physical limits (maximum suspension deflection $| x_s - x_u |_{\max}$, body acceleration $\ddot{x}_s$, and control force $| u |_{\max}$) to balance the ride comfort and actuation effort. After normalization, Q and R are iteratively tuned to achieve low RMS body acceleration while maintaining bounded peak control force.

The LQR controller guarantees the asymptotic stability of the closed-loop system when the pair (A, B_u) is controllable. However, its performance strongly depends on fixed weighting matrices, which limit its adaptability when disturbance levels vary significantly.

B. H∞ Controller

To enhance robustness against disturbances and model uncertainties, the H∞ control problem is formulated using the generalized plant representation:

$$\dot{x} = Ax + B_1 w + B_2 u, \quad z = C_1 x + D_{12} u, \quad y = C_2 x \quad (8)$$

The objective is to design a state-feedback control law:

$$u = -K_\infty x$$

such that the H∞ norm of the transfer function from disturbance w to performance output z satisfies:

$$\left\| T_{w \to z} \right\|_\infty < \gamma \quad (9)$$

with $\gamma > 0$ as small as possible.

The performance output is weighted as:

$$z = \begin{bmatrix} W_1 \left(x_s - x_u \right) \\ W_2 \ddot{x}_s \\ W_3 u \end{bmatrix} \quad (10)$$

where:

- W_1: suspension travel limitation (mechanical safety)
- W_2: ride comfort priority (body acceleration)
- W_3: actuator effort constraint

To select these weights, they were first normalized according to the physical limits:

$$W_1 = \frac{1}{\Delta x_{max}}, \quad W_2 = \frac{1}{a_{s,max}}, \quad W_3 = \frac{1}{u_{max}} \quad (11)$$

Subsequently, iterative tuning is performed: W_2 is increased if the RMS body acceleration remains high; W_3 is increased if the peak control force exceeds the limit; and W_1 is adjusted to avoid suspension bottoming.

The gain matrix K_∞ is obtained by solving standard H∞ Riccati equations. In the simulations, $\gamma \leq 1.5$ is maintained across all disturbance scenarios.

H∞ control guarantees worst-case disturbance attenuation; however, it typically generates larger control forces and a relatively stiff response under mild excitation.

C. Proposed Adaptive Fuzzy–LQR (AF–LQR)

To overcome the rigidity of classical LQR with fixed weighting matrices and the tendency of H∞ control to generate large actuation forces under mild disturbances, the proposed method adjusts the LQR gain according to the instantaneous vibration level of the system.

The proposed control law is:

$$u(t) = -\beta(t) K x(t) \quad (12)$$

where K is the optimal LQR gain matrix and $\beta(t)$ is an adaptive scaling factor determined by a fuzzy inference mechanism.

1) Fuzzy Inference Mechanism

Two input variables were selected to directly reflect the vibration performance:

- Suspension deflection: $e_1 = \Delta x = x_s - x_u$
- Body acceleration: $e_2 = a_s = \ddot{x}_s$

These variables were chosen because e_1 is directly related to the mechanical suspension limits, while e_2 reflects passenger ride comfort.

To eliminate unit dependency, the variables are normalized as:

$$\tilde{e}_1 = \frac{e_1}{e_{1,\max}}, \quad \tilde{e}_2 = \frac{e_2}{e_{2,\max}}$$

where $e_{1,\,max}$ = 0.08 m (maximum suspension travel) and $e_{1,\,max}$ = 3 m/s^2 (acceptable acceleration threshold).

Thus:

$$\tilde{e}_1, \tilde{e}_2 \in [-1,\ 1] \quad (13)$$

After normalization, each input variable was divided into five symmetric fuzzy sets: Negative Big (NB), Negative Small (NS), Zero (ZO), Positive Small (PS), and Positive Big (PB), as defined in Table I.

TABLE I. NORMALIZED MEMBERSHIP FUNCTION RANGES

Label	Meaning	Normalized range
NB	Negative Big	[-1, -0.5]
NS	Negative Small	[-0.8, 0]
ZO	Zero	[-0.3, 0.3]
PS	Positive Small	[0, 0.8]
PB	Positive Big	[0.5, 1]

Triangular membership functions were employed with a 50% overlap.

The output variable $\beta \in [\beta_{min}, \beta_{max}] = [0.6, 1.8]$ is divided into three linguistic levels, as shown in Table II.

TABLE II. OUTPUT LINGUISTIC VALUES

Label	Sugeno values
S (Small)	0.7
M (Medium)	1.0
L (Large)	1.5

A zero-order Sugeno model was adopted to ensure fast computation and suitability for real-time implementation. The output scaling factor is computed as:

$$\beta = \frac{\sum w_i \beta_i}{\sum w_i} \quad (1)$$

The fuzzy rule base, as illustrated in Table III, follows these principles:

- If suspension deflection and acceleration are large, then $\beta = L$ (strong control action).
- If the road is smooth (ZO, ZO), then $\beta = S$ (reduced control effort).
- For intermediate conditions: $\beta = M$.

TABLE III. FUZZY RULE BASE

$e_2 \backslash e_1$	NB	NS	ZO	PS	PB
NB	L	L	M	S	S
NS	L	M	M	S	S
ZO	M	M	S	M	M
PS	S	S	M	M	L
PB	S	S	M	L	L

2) Bounded Adaptation and Stability Analysis

The adaptive gain is constrained as:

$$\beta_{min} \le \beta(t) \le \beta_{max} \quad (15)$$

with $0 < \beta_{\min} < 1 < \beta_{\max}$.

Consider the Lyapunov candidate function:

$$V(x) = x^T P x \quad (16)$$

where P is the positive definite solution of the LQR Riccati equation.

Substituting the control law (12) into the closed-loop system yields:

$$\dot{x} = (A - \beta BK)x + B_w w \quad (17)$$

Since $\beta(t)$ is bounded and K stabilizes the system when $\beta = 1$, there are positive constants α_1, α_2 such that:

$$\dot{V} \le -\alpha_1 \| x \|^2 + \alpha_2 \| w \|^2 \quad (18)$$

Therefore, the closed-loop system satisfies the Input-to-State Stability (ISS) property. This guarantees that:

- If the disturbance is bound, the system states remain bounded.
- If the disturbance diminishes, the system states converge asymptotically.

3) Algorithm 1: AF–LQR Design and Implementation

Input: System matrices A, B_u, B_w ; physical limits $\Delta x_{\max}, a_{s,\max}, u_{\max}$.
Output: Adaptive control law $u(t) = -\beta(t)Kx(t)$.

a) Step 1: Nominal LQR Design

Select normalized weighting matrices $Q \succeq 0$, $R \succ 0$. Solve the algebraic Riccati equation and compute $K = R^{-1} B_u^T P$.

b) Step 2: Signal Normalization

Set $e_{1,\max} = \Delta x_{\max}$, $e_{2,\max} = a_{s,\max}$. Compute normalized inputs $\tilde{e}_1, \tilde{e}_2 \in [-1, 1]$.

STEP 3: FUZZY INFERENCE CONSTRUCTION

Define triangular membership functions (NB, NS, ZO, PS, PB). Establish the fuzzy rule base. Adopt a zero-order Sugeno inference model.

c) Step 4: Bounded Gain Adaptation

Choose $\beta_{\min}$ and $\beta_{\max}$ such that:

$0 < \beta_{\min} < 1 < \beta_{\max}$.
Compute the adaptive gain $\beta(t) = \frac{\sum w_i \beta_i}{\sum w_i}$.

d) Step 5: Performance Verification and Tuning

Evaluate RMS body acceleration, peak control force, and ISE of suspension deflection. Adjust fuzzy rules and parameters if necessary.

IV. SIMULATION SETUP

A. ISO 8608 Road Profiles (A–D)

The spatial PSD is defined as:

$$G_q(n) = G_q(n_0)\left(\frac{n}{n_0}\right)^{-2} \quad (18)$$

where $G_q(n_0)$ specifies the roughness level at the reference spatial frequency for each ISO 8608 class, as presented in Table IV.

TABLE IV. ISO 8608 (A–D) PAVEMENT

Class	$G_q(n_0)$	Description
A	16.10^{-6}	Very smooth highway surface
B	64.10^{-6}	Smooth road with minor irregularities
C	256.10^{-6}	Typical urban/provincial road
D	1024.10^{-6}	Rough or degraded road surface

A time-domain road signal $r(t)$ was generated using the spectral synthesis method.

B. Simulation Parameters

The simulation parameters were set as follows: sprung mass $m_b = 973$ kg, unsprung mass $m_w = 114$ kg, suspension stiffness $k_s = 32720$ N/m, suspension damping coefficient $b_s = 1095$Ns/m, tire stiffness $k_t = 81115$N/m, and a vehicle speed of 72 km/h. The simulation times were 2 s for the bump input and 5 s for the ISO-C road profile, with a sampling time of 0.001 s. The H∞ weighting parameters were selected as: $W_1 = 12.5; W_2 = 0.333; W_3 = 2.510^{-4}$.

V. RESULTS AND DISCUSSION

The performance of the proposed AF–LQR controller was evaluated under both deterministic and stochastic road excitations, followed by a robustness analysis with respect to parameter uncertainties. The results demonstrate the ability of the adaptive strategy to achieve a balanced trade-off among ride comfort, suspension safety, and control effort. Under impulsive disturbance, the half-sine bump profile displayed in Figure 2 was used to evaluate transient behavior. Figure 3 shows that all active controllers reduced vibration compared with the passive suspension. LQR and AF–LQR suppressed oscillations and reduced settling time, while the H∞ controller achieved the lowest peak amplitude with a more aggressive response.

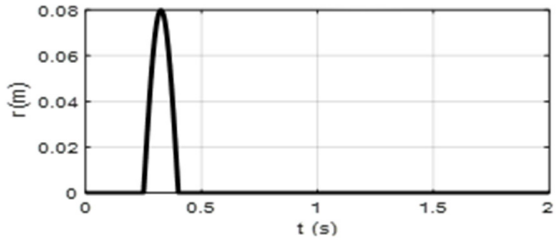

Fig.2. Half-sine bump road profile.

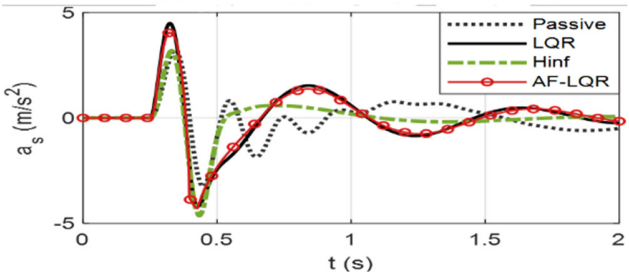

Fig.3. Body acceleration comparison.

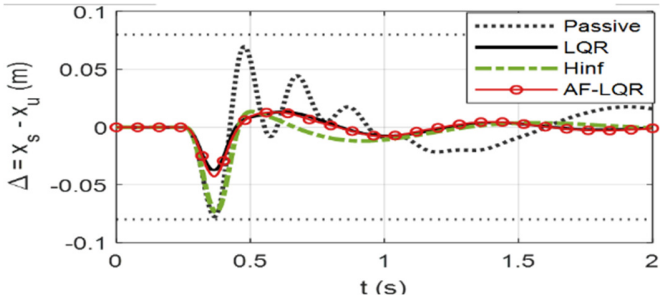

Fig.4. Suspension deflection comparison.

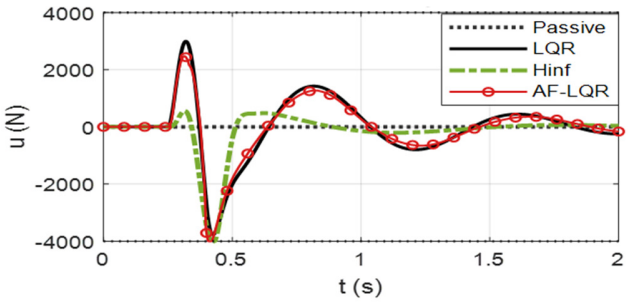

Fig.5. Control force comparison.

This behavior is further clarified by the suspension deflection results in Figure 4, where AF–LQR maintains a deflection within bounds comparable to LQR and notably lower than H∞. Meanwhile, the control force profiles in Figure 5 reveal that AF–LQR produces smoother actuation signals, whereas H∞ introduces rapid and high-amplitude variations, which may be undesirable in practical applications.

These observations are quantitatively supported in Table V, where AF–LQR reduces RMS body acceleration from 1.9435 m/s² (passive) to 1.2621 m/s², closely matching LQR (1.3141 m/s²) while maintaining low suspension deflection. Although H∞ achieves the lowest RMS value (0.9798 m/s²), this improvement is accompanied by increased suspension travel and higher control effort. This confirms that AF–LQR provides a more balanced compromise, avoiding excessive actuation while still achieving substantial vibration attenuation.

TABLE V. PERFORMANCE METRICS UNDER BUMP EXCITATION

Method	RMS(a_s)(m/s²)	RMS(Δ) (m)	Max |U| (N)
Passive	1.9435	0.0231	0
LQR	1.3141	0.0088	3772.5
AF-LQR	1.2621	0.0095	4000
H∞	0.9798	0.0154	4000

The advantages of the proposed method become more evident under stochastic excitation. The ISO 8608 Class C road profile illustrated in Figure 6 introduces broadband disturbances that better reflect real driving conditions. As exhibited in Figure 7, AF–LQR consistently achieved lower body acceleration than LQR, with smoother temporal variations. The suspension deflection results in Figure 8 further demonstrate that AF–LQR maintains minimal displacement levels, whereas H∞ exhibits larger excursions due to its

aggressive disturbance rejection mechanism. Similarly, the control force responses in Figure 9 confirm that AF–LQR operates with moderate and stable actuation, in contrast to the oscillatory behavior observed in H∞.

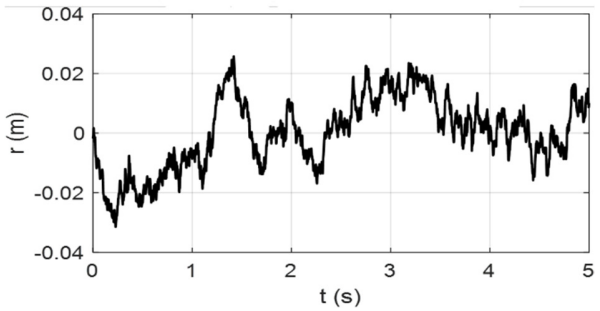

Fig. 6. ISO 8608 Class C road profile generated using the spectral synthesis method.

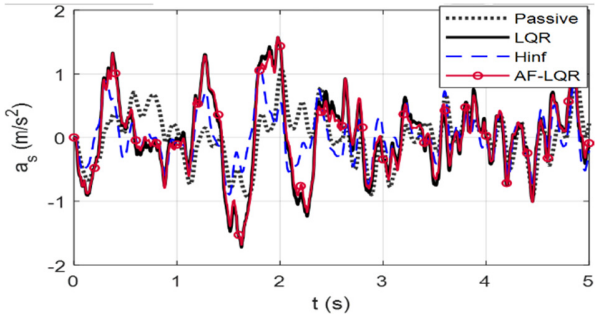

Fig. 7. Body acceleration responses of the compared controllers under ISO 8608 Class C excitation.

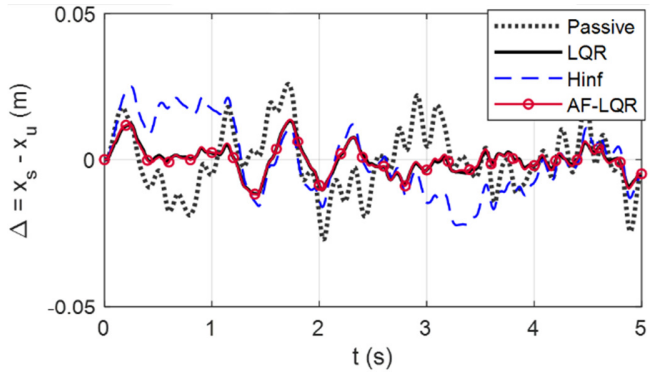

Fig. 8. Suspension deflection comparison.

The numerical results in Table VI support these findings. AF–LQR reduces RMS body acceleration to 0.6134 m/s², achieving approximately 4% improvement over LQR while maintaining the lowest suspension deflection (0.0050 m) among all active methods. Although H∞ achieves superior vibration reduction (0.3776 m/s²), this comes at the cost of significantly larger suspension motion. These results highlight the effectiveness of the adaptive gain factor β(t), which adjusts the control intensity according to the disturbance level, enabling disturbance-dependent behavior that cannot be achieved using fixed-gain controllers.

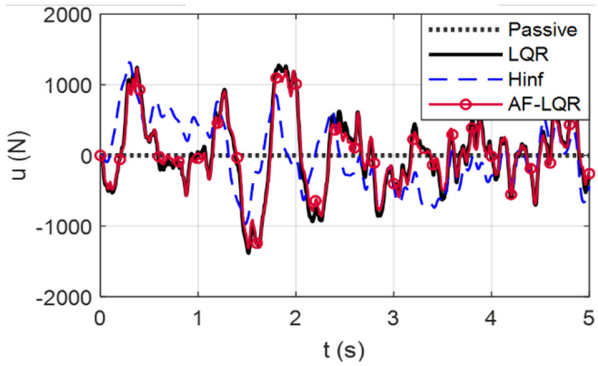

Fig. 9. Control force comparison.

TABLE VI. PERFORMANCE METRICS UNDER ISO 8608 CLASS C

Method	RMS(a_s)(m/s^2)	RMS(Δ) (m)	Max |U| (N)
Passive	1.4109	0.0110	0
LQR	0.6396	0.0050	1385.4
AF-LQR	0.6134	0.0050	1314.4
H∞	0.3776	0.0123	1319.7

To further evaluate the robustness, the system parameters were varied within ±20%, and the results are summarized in Tables VII–XII. Across all scenarios, AF–LQR maintained a stable performance with only minor deviations from the nominal conditions. The RMS body acceleration varied within a narrow range (approximately 3–6%), and the suspension deflection remained within the mechanical safety limits. In contrast, LQR exhibits more noticeable performance degradation in certain cases owing to its fixed weighting structure. Tables VII-XII outline the performance metrics for different parameter variations.

TABLE VII. ISO 8608-C WITH m_s INCREASED BY 20%

Method	RMS(a_s)(m/s^2)	RMS(Δ) (m)	Max |U| (N)
Passive	1.4415	0.0148	0
LQR	0.4807	0.0049	1290.6
AF-LQR	0.4512	0.0050	1203.3
Hinf	0.2956	0.0072	858.8033

TABLE VIII. ISO 8608-C WITH m_s DECREASED BY 20%

Method	RMS(a_s)(m/s^2)	RMS(Δ) (m)	Max |U| (N)
Passive	1.4368	0.0090	0
LQR	0.9081	0.0049	1662.5
AF-LQR	0.9019	0.0050	1652.0
H∞	0.4544	0.0111	1186.0

TABLE IX. ISO 8608-C WITH k_s INCREASED BY 20%

Method	RMS(a_s)(m/s^2)	RMS(Δ) (m)	Max |U| (N)
Passive	1.4065	0.0091	0
LQR	0.6803	0.0048	1466.3
AF-LQR	0.6587	0.0048	1410.4
H∞	0.3848	0.0116	1416.3

TABLE X. ISO 8608-C WITH k_s DECREASED BY 20%

Method	RMS(a_s)(m/s^2)	RMS(Δ) (m)	Max |U| (N)
Passive	1.4183	0.0140	0
LQR	0.6020	0.0052	1.307.5
AF-LQR	0.5712	0.0052	1224.4
H∞	0.3428	0.0084	944.9332

TABLE XI. ISO 8608-C WITH b_s INCREASED BY 20%

Method	RMS(a_s)(m/s^2)	RMS(Δ) (m)	Max |U| (N)
Passive	1.4002	0.0104	0
LQR	0.6491	0.0049	1386.6
AF-LQR	0.6224	0.0049	1320.1
H∞	0.3564	0.0107	1145.6

TABLE XII. ISO 8608-C WITH b_s DECREASED BY 20%

Method	RMS(a_s)(m/s^2)	RMS(Δ) (m)	Max |U| (N)
Passive	1.4282	0.0118	0
LQR	0.6313	0.0050	1388.0
AF-LQR	0.6058	0.0051	1312.6
H∞	0.3626	0.0076	1076.9

Moreover, AF–LQR consistently achieves lower RMS acceleration than LQR while maintaining comparable or lower control efforts. Although the peak control force slightly increased in some cases (e.g., reduced sprung mass), it remained within the predefined saturation limits, confirming the effectiveness of the bounded adaptation mechanism. Compared to the H∞ control, AF–LQR demonstrated improved energy efficiency and smoother actuation while preserving a robust disturbance rejection capability.

Overall, the results indicate that the proposed AF–LQR controller effectively combines the advantages of optimal control and adaptive strategy. Although H∞ control provides strong worst-case performance, it tends to generate excessive control effort and larger suspension deflection. However, the classical LQR lacks flexibility under varying disturbances. The AF–LQR approach bridges this gap by introducing a bounded adaptive gain mechanism that enhances adaptability without increasing computational complexity.

From a practical perspective, the proposed method is particularly suitable for real-time automotive applications, as it ensures stable performance under realistic road conditions while maintaining actuator constraints and computational efficiency. These characteristics make AF–LQR a promising solution for next-generation active suspension systems.

VI. CONCLUSION AND FUTURE WORK

This paper proposed an Adaptive Fuzzy– Linear Quadratic Regulator (AF–LQR) control strategy for a quarter-car active suspension system operating under both deterministic and stochastic road excitations. The proposed method integrates the optimal structure of Linear Quadratic Regulator (LQR) with a bounded fuzzy-based gain adaptation mechanism, enabling real-time adjustment of control intensity based on suspension deflection and body acceleration.

Unlike conventional fixed-gain controllers, the proposed approach introduces a disturbance-dependent adaptive scaling factor, which allows the controller to dynamically balance ride comfort, suspension safety, and control effort. Theoretical analyses ensured that the closed-loop system satisfies Input-to-State Stability (ISS) under bounded disturbances, providing a formal guarantee of robustness.

Extensive simulations under both bump excitation and ISO 8608 Class C road profiles demonstrated that the AF–LQR controller consistently achieved improved vibration attenuation compared to classical LQR, while maintaining tight suspension deflection bounds and smoother control signals. Although H∞ control provided stronger worst-case disturbance rejection, it exhibited larger suspension excursions and more aggressive actuation, which may limit its practical applicability. In contrast, the proposed AF–LQR achieved a more balanced and practically feasible trade-off.

Furthermore, robustness analyses under ±20% parameter variations confirmed that the proposed controller maintained stable and consistent performance with only minor degradation. This robustness is primarily attributed to the bounded adaptive mechanism, which preserves system stability while avoiding excessive control effort.

Overall, this study bridges the gap between optimal control and adaptive intelligent strategies, providing a computationally efficient, physically interpretable, and implementation-oriented solution for active suspension systems. The proposed AF–LQR framework is particularly suitable for real-time automotive applications, where performance, robustness, and actuator constraints must be simultaneously satisfied.

Future work will focus on extending the proposed approach to half-car and full-car models to capture pitch and roll dynamics, as well as incorporating energy-aware and actuator-constrained optimization. In addition, the integration of learning-based tuning methods for automatic adaptation of fuzzy parameters will be investigated. Finally, experimental validation, including Hardware-in-the-Loop (HIL) or real-vehicle testing, is considered a critical step toward practical deployment.

DECLARATION OF COMPETING INTERESTS

The authors declare that they have no known competing financial interests or personal relationships that could have appeared to influence the work reported in this paper.

ACKNOWLEDGMENT

The authors wish to thank the Thai Nguyen University of Technology for supporting this work.

DATA AVAILABILITY

The data supporting the findings of this study are generated through numerical simulations of the proposed quarter-car suspension model under ISO 8608 road profiles and can be available from the corresponding author upon reasonable request.

REFERENCES

[1] K. Arunachalam, P. Jawahar, and P. Tamilporai, "Active Suspension System with Preview Control - A Review," SAE Technical Paper 2003-28-0037, https://doi.org/10.4271/2003-28-0037.

[2] J. Cao, H. Liu, P. Li and D. J. Brown, " State of the Art in Vehicle Active Suspension Adaptive Control Systems Based on Intelligent Methodologies," *IEEE Transactions on Intelligent Transportation Systems*, vol. 9, no. 3, pp. 392-405, Sep. 2008, https://doi.org/10.1109/TITS.2008.928244.

[3] I. Jiregna and G. Sirata, "A Review of the Vehicle Suspension System," *Journal of Mechanical and Energy Engineering*, vol. 4, no. 2, pp. 109-114, Jun. 2020, https://doi.org/10.30464/jmee.2020.4.2.109.

[4] F. Rana, "Types and application of advance suspension system," *International Journal of Automobile Engineering,* vol. 5, no. 2, pp. 01-07, Jul. 2024, https://doi.org/10.22271/27078205.2024.v5.i2a.34.

[5] A. A. Ferhath and K. Kamalakkannan, "A Review on Various Control Strategies and Algorithms in Vehicle Suspension Systems," *International Journal of Automotive and Mechanical Engineering*, vol. 20, no. 3, pp. 10720-10735, Oct. 2023, https://doi.org/10.15282/ijame.20.3.2023.14.0828.

[6] J. Theunissen, A. T. P. Gruber, M. Dhaens and A. Sorniotti, "Preview-based techniques for vehicle suspension control: a state-of-the-art review," *Annual Reviews in Control*, vol. 51, pp. 206-235, Jan. 2021, https://doi.org/10.1016/j.arcontrol.2021.03.010.

[7] S. Rozali, M. N. Kamarudin, S. M. Saleh and A. C. Amran, "Linear Quadratic Regulator Design for Vehicle Suspension System," *ARPN Journal of Engineering and Applied Sciences*, vol. 17, no. 1, Jan. 2022.

[8] K. D. Dandavate and P. R. Kale, "A Review on Controlling Methods for Active Suspension Systems," *International Journal for Research in Applied Science and Engineering Technology,* vol. 11, no. 11, pp. 1675-1680, Nov. 2023, https://doi.org/10.22214/ijraset.2023.56929.

[9] W. A. Ashtari, "Enhancing the Performance of Active Suspension Systems Through Adaptive Control," *European Journal of Automated Systems,* vol. 57, no. 3, pp. 887-897, Jun. 2024, https://doi.org/10.18280/jesa.570328.

[10] F. Zhao, S. S. Ge, F. Tu, Y. Qin and M. Dong, "Adaptive neural network control for active suspension system with actuator saturation" *IET Control Theory and Applications,* vol. 10, no. 14, pp. 1696-1705, Sep. 2016, https://doi.org/10.1049/iet-cta.2015.1317.

[11] S. Chantranuwathana and H. Peng "Adaptive Robust Control for Active Suspension," *Proceedings of the American Control Conference*, San Diego, CA, USA, Jun. 1999, pp. 1702-1706, https://doi.org/10.1109/ACC.1999.786126.

[12] D. Karnopp, "Active damping in road vehicle suspension systems," *Vehicle System Dynamics*, vol. 12, no. 6, pp. 291-311, Jul. 2007, https://doi.org/10.1080/00423118308968758.

[13] G. Li *et al.*, "Research on LPV-H∞ control strategy of magnetorheological semi-active suspension with air spring," *Scientific Reports*, vol. 15, no. 1, 2025, Art. no. 39206, https://doi.org/10.1038/s41598-025-15552-1.

[14] K. Yeneneh, M. Walle, T. Mamo and Y. Yalew, "Optimizing active suspension systems with robust h∞ control and adaptive techniques under uncertainties," *Applications in Engineering Science*, vol. 22, Jun. 2025, Art. no. 100225, https://doi.org/10.1016/j.apples.2025.100225.

[15] D. Savaresi, F. Favalli, S. Formentin and S. M. Savaresi, "On-line Damping Estimation in Road Vehicle Semi-active Suspension Systems," *IFAC PapersOnLine*, vol. 52, no. 5, pp. 679-684, Jan. 2019, https://doi.org/10.1016/j.ifacol.2019.09.108.

[16] Z. Yang, C. Yong, Z. Li and Y. Kangsheng, "Simulation analysis and optimization of ride quality of in-wheel motor electric vehicle," *Advances in Mechanical Engineering*, vol. 10, no. 5 pp. 01-10, 2018, https://doi.org/10.1177/1687814018776543.

[17] L. Zhang , S. Zhang and W. Zhang, "Multi-objective optimization design of in-wheel motors drive electric vehicle suspensions for improving handling stability," *Proceedings of the Institution of Mechanical Engineers Part D Journal of Automobile Engineering*, vol. 233, no. 8, pp. 2232-2245, Jun. 2018, https://doi.org/10.1177/0954407018783145.

[18] D. T. Tu, "Enhancing Road Holding and Vehicle Comfort for an Active Suspension System Utilizing Model Predictive Control and Deep Learning," *Engineering, Technology & Applied Science Research*, vol. 14, no. 1, pp. 12931-12936, Feb. 2024, https://doi.org/10.48084/etasr.6582.

[19] P. Múčka, "Simulated Road Profiles According to ISO 8608 in Vibration Analysis," *Journal of Testing and Evaluation*, vol. 46, no. 1, pp. 90-3973, Jan. 2018, https://doi.org/10.1520/JTE20140493.